

New integral equation theory for primitive model ionic liquids: From electrolytes to molten salts

C. Satheesan Babu and Toshiko Ichiye

Citation: *The Journal of Chemical Physics* **100**, 9147 (1994); doi: 10.1063/1.466669

View online: <http://dx.doi.org/10.1063/1.466669>

View Table of Contents: <http://scitation.aip.org/content/aip/journal/jcp/100/12?ver=pdfcov>

Published by the [AIP Publishing](#)

Articles you may be interested in

The mean activity coefficients of 2:2 electrolyte solutions: An integral equation study of the restricted primitive model

J. Chem. Phys. **130**, 134513 (2009); 10.1063/1.3099335

Integral equation theory of flexible polyelectrolytes. II. Primitive model approach

J. Chem. Phys. **111**, 6633 (1999); 10.1063/1.479953

Integral equation theory for charged liquids: Model 2–2 electrolytes and the bridge function

J. Chem. Phys. **97**, 7716 (1992); 10.1063/1.463491

Ionic adsorption from a primitive model electrolyte—nonlinear treatment

J. Chem. Phys. **75**, 3485 (1981); 10.1063/1.442458

Exact Solution of an Integral Equation for the Structure of a Primitive Model of Electrolytes

J. Chem. Phys. **52**, 4307 (1970); 10.1063/1.1673642



New integral equation theory for primitive model ionic liquids: From electrolytes to molten salts

C. Satheesan Babu and Toshiko Ichiye^{a)}

Departments of Biochemistry/Biophysics and Chemistry, Washington State University, Pullman, Washington 99164-4660

(Received 19 January 1994; accepted 8 March 1994)

A new closure to the Ornstein–Zernike (OZ) equation is proposed for ionic liquids and is investigated for primitive models of high valency (2:2) aqueous electrolyte solutions and molten salts. The new closure, which is related to an earlier closure for the soft-sphere case proposed by Ichiye and Haymet, may be viewed as a prescription for the so-called “bridge functions.” These functions are approximated by zero in the hypernetted-chain (HNC) closure which is generally used for ionic systems. In both the new closure and the soft-sphere closure, the recognition that the unlike bridge function is opposite in sign from the like bridge function leads to an approximation for these missing graphs by adding (for the unlike case) or subtracting (for the like case) a set of graphs similar to those used in Percus–Yevick theory to the HNC equation. Compared to the HNC closure, the pair correlation functions predicted for primitive models by the new closure are generally in much better agreement with Monte Carlo (MC) simulations of molten salts and aqueous 2:2 electrolytes. The fundamental improvement of this paper over the Ichiye–Haymet work is that the separation of long- and short-range part of $c(r)$ for the hard-sphere case is clearly defined, whereas it was done numerically for the soft-sphere case. Moreover, the present theory is in better agreement with MC simulations both in the molten salt as well as in the dilute solution regimes than the soft-sphere case. Finally, a study was made of the transition of the like charge pair correlation functions from monotonic behavior at low densities to a nonmonotonic behavior at high densities. The new closure clearly predicts such a transition region at concentrations near 0.02 M and temperatures near 314 K. There is also a region below 0.02 M and 314 K where the new closure fails to converge. Compared to MC simulations, the critical region predicted by the new closure appears to be a lower estimate. However, for the HNC closure there is only a remote possibility of such a transition region since the correlation functions are nonmonotonic even at lower concentrations, a feature which is corrected in the new theory.

I. INTRODUCTION

The development of an accurate theory of ionic solutions is crucial to understanding chemical and biochemical processes such as electron transfer^{1,2} and protein folding.³ Traditionally, one can get qualitative ideas regarding the behavior of ionic distribution functions from the Debye–Hückel theory for dilute solutions or from the Poisson–Boltzmann equation. However, the most successful theories of electrolyte solutions are those based on the Ornstein–Zernike (OZ) equation⁴ with appropriate closure relations.^{5–7} The hypernetted-chain (HNC) closure is regarded as the best closure relation for ionic systems such as electrolyte solutions over a wide range of thermodynamic state points,^{6,8} molten salts,^{7,9} and one component plasmas.⁷ However, HNC theory fails when it is used to compute the distribution functions in highly associating ionic solutions such as 2:2 electrolyte solutions at extremely low concentrations (typically 10^{-1} to 10^{-4} M).^{10–12} In these systems, Monte Carlo (MC) simulations revealed the presence of ion pairs and larger ionic clusters.^{10,11} The theory predicts a local maximum for the like ion pair distribution function at $r=2R$, where R is the contact distance of the ion pairs, which is contrary to the expected monotonic behavior of distribution functions in

these systems. From MC simulations of the same systems, the local maximum in the like ion distribution functions appears to be an artifact of the HNC theory.^{10,11} The HNC equation also underestimated the height of the unlike charge pair distribution function in these systems. In addition, although HNC theory is convergent in the molten salt regime and predicts qualitatively reasonable $g(r)$'s, there are some discrepancies especially for hard spheres. For hard-sphere models of molten salts, the HNC equation overestimates the unlike charge pair distribution function, while for the like charges, the HNC underestimates the first peak and overestimates the small peak at $r=2R$ as compared to the corresponding MC data.¹³ Finally, the HNC equation severely overestimates the first peaks of OH and HH radial distribution functions in a central force model (CFM) of liquid water,^{14,15} in which water is treated as a two component mixture of O and H.^{16–19}

The failure of HNC theory in the above-mentioned cases is due to the neglect of a set of diagrams called the bridge diagrams in the cluster expansion of the pair distribution functions.²⁰ Inclusion of the first bridge graph, which was numerically integrated in the HNC equation dramatically improved the quality of distribution functions for dilute 2:2 electrolytes.^{10,11} There has also been interest in incorporating hard-sphere bridge functions into the HNC equation based on the idea of the universality of the bridge functions.^{21–23}

^{a)} Author to whom correspondence should be addressed.

This results in considerable improvement in the molten salt regime for hard spheres,¹³ especially when different diameters are used for the reference hard-sphere bridge functions for the like and unlike pairs.²⁴ More recently, Ichiye and Haymet²⁵ proposed a new closure for ionic fluids, referred to here as the ionic PY (IPY) closure, which is related to the Percus–Yevick (PY) closure but was based on the idea that ++ bridge function is opposite in sign from that of the +−bridge function.^{26,27} Another ingredient of the closure was the separation of the long- and short-range parts of the potential. Since the IPY closure was designed for soft spheres, the long-range part of the potential is treated as a generalization of the mean spherical approximation (MSA) chain sums.²⁸ It is thus related to the Allnatt's modification of the PY closure (PYA)²⁹ and to the work of Rogde and Hafskjold.^{12,30} The IPY closure generally gives considerable improvement over the HNC closure for dilute strong soft-sphere electrolytes.^{25,31,32} It correctly predicts no peak in the like $g(r)$ at 0.005 M (whereas the HNC incorrectly predicts a peak) and gives peaks for the unlike $g(r)$ between 0.005 and 0.2 M which are much closer to MC than the HNC. However, at concentrations of 0.0625 and 0.2 M, the IPY results for the like charges were in slightly worse agreement with the MC data than the simple HNC. In all cases, the IPY results were similar to or better than those including the numerically integrated first bridge graph.^{10,11} A major failure of this previous IPY closure is that it gives no improvement over the HNC results in the molten salt regime.

The work presented here is for a more specialized case than in the previous work, namely, that of hard spheres. This allows us to improve over the previous IPY closure in that a closed form for the long-range potential can be formulated, namely, the standard MSA chain sums, thus making the computation easier and the separation of the short- and long-range potentials more distinct. The previous work involved an additional step in which the long-range potential was solved numerically. Moreover, the present closure is an improvement over the IPY closure because it gives better results than HNC both in the molten salt as well as in the dilute aqueous solution regimes. The present system of hard spheres has identical thermodynamic properties such as excess free energies and osmotic coefficients as in the previous work on the soft-sphere model.²⁵ For a detailed discussion of the similarities between the two models, the reader is referred to the work of Rossky *et al.*¹⁰ The transition between the monotonic behavior of the like charge distribution functions at low concentrations to the nonmonotonic behavior at high concentrations is also studied.

The quality of distribution functions obtained from theories can be assessed by comparing these results with MC or molecular dynamics (MD) data for the same model systems. MC simulations³³ are widely employed for studying systems of hard spheres with Coulomb tails primarily because of the difficulty in MD simulations of predicting hard-sphere collision times in these systems.³⁴ We have performed MC simulations in each of the electrolyte concentrations studied with integral equation theory. The present MC calculations differ from the previous MC simulations^{10,11,13} in that the present calculations are performed for hard spheres instead of soft

spheres and with a greater number of trial moves, thus giving better averages than the previous ones.

We briefly describe our notation for the Ornstein–Zernike equation for mixtures, the renormalization for the charged systems, and our rationale for our new closure for the Ornstein–Zernike equation in Sec. II. In Sec. III, we describe our MC simulations and in Sec. IV, we present comparisons of our new closure with MC simulation data for molten salt and various concentrations of ionic solutions. Finally, we present a brief discussion of those results and our major conclusions.

II. THEORY

The general details for the methods used to solve the integral equations and the renormalization are presented elsewhere.^{14,25} In Sec. II A, we summarize renormalized integral equations for mixtures and standard closures following our previous notation. In Sec. II B, we present the new closure.

A. Integral equations for ionic mixtures

We consider particles interacting via pair potentials $u_{ab}(r)$ where the subscripts denote the species. The Ornstein–Zernike equation for the pair correlation function for mixtures is

$$h_{ab}(r) = c_{ab}(r) + \sum_s \rho_s c_{as}^* h_{sb}(r), \quad (2.1)$$

where $g_{ab} = h_{ab} + 1$ is the pair correlation function, c_{ab} is the direct correlation function, and ρ_s is the number density of species s and $*$ denotes a convolution. (We omit reference to the argument r when it is unambiguous.) Defining a matrix ρ with elements $\rho_{ab} = \rho_a \delta_{ab}$, we may write Eq. (2.1) as

$$\rho \hat{\mathbf{t}} \rho = \rho \hat{\mathbf{c}} \rho \hat{\mathbf{h}} \rho, \quad (2.2)$$

where $\mathbf{t} = \mathbf{h} - \mathbf{c}$ and the caret denotes a Fourier transform.

For the renormalization, we define

$$\phi_{ab}(r) = -\beta u_{ab}(r) + \beta u_{ab}^s(r), \quad (2.3)$$

where u_{ab}^s is the short-range part of the potential and $\beta = 1/k_B T$, in which k_B is the Boltzmann constant and T is the temperature. For example, the interparticle potential function for the primitive electrolyte model with particle diameter R may be written as

$$u_{ab}(r) = \begin{cases} \infty & r < R, \\ -\frac{Z_a Z_b}{\epsilon r} & r > R, \end{cases} \quad (2.4)$$

where a and b are species labels which take on values + and −, Z_a is the charge for species a , and ϵ is the bulk dielectric constant. For Coulombic systems such as this, ϕ_{ab} [Eq. (2.3)] is usually chosen to be

$$\phi_{ab}(r) = -\beta \frac{Z_a Z_b}{\epsilon r}. \quad (2.5)$$

The renormalized Ornstein–Zernike equation is then

$$\rho \hat{\mathbf{t}} \rho = \hat{\mathbf{V}} \mathbf{c} [\mathbf{I} - \hat{\mathbf{V}} \mathbf{c}^s]^{-1} \hat{\mathbf{V}} - \rho \hat{\mathbf{c}}^s \rho, \quad (2.6)$$

where $\mathbf{V}^{-1} = \rho^{-1} - \phi$, $\mathbf{c}^s = \mathbf{c} - \phi$, $\tau = \mathbf{t} - \mathbf{q} + \phi$, and $\rho \mathbf{q} \rho = \mathbf{V} - \rho$. For Coulombic systems, q_{ab} is given by

$$q_{ab}(r) = -\beta \frac{Z_a Z_b}{\epsilon r} e^{-\kappa r}, \quad (2.7)$$

where $\kappa^2 = 4\pi\beta\epsilon^{-1}\sum_a \rho_a Z_a^2$ is the Debye screening constant.

The exact renormalized closure may be written as

$$c_{ab}^s = \exp(-\beta u_{ab}^s + \tau_{ab} + q_{ab} + B_{ab}) - 1 - \tau_{ab} - q_{ab}, \quad (2.8)$$

where B_{ab} is the bridge function. The function B_{ab} can be expressed diagrammatically as all simple diagrams consisting of two white 1-circles labeled 1 and 2, black $\rho^{(1)}$ circles, and f -bonds where $f_{ab} = \exp(-\beta u_{ab}) - 1$, such that the white circles are not an articulation pair and there is no $f(1,2)$ -bond and such that they are free of nodal circles.⁷ Closure relations such as PY and HNC involve different approximations for B_{ab} .⁷ For instance, the PYA approximation is

$$B_{ab}^{\text{PYA}} = \log(1 + \tau_{ab}) - \tau_{ab}, \quad (2.9a)$$

where ϕ_{ab} , q_{ab} , and τ_{ab} are defined as in Eqs. (2.5)–(2.7) and which reduces to the PY approximation when $\phi_{ab} = 0$. The HNC approximation is

$$B_{ab}^{\text{HNC}} = 0. \quad (2.9b)$$

It is well known that, in general, the PY approximation is better for short-ranged repulsive forces, despite the fact that it includes fewer diagrams in h and c . This can be understood graphically because the largest contributions to the first bridge graph are at small separations. In this region, the f bonds are approximately -1 for separations within the repulsive core and close to zero elsewhere. Thus, the graphs in h and c neglected in PY but included in HNC are those which are canceled by B (up to ρ^2). The HNC closure has been found to be effective for systems with long-range forces. However, as described in the introduction, the HNC approximation begins to break down in systems where charge association occurs. Presumably, the short-range forces which are better handled by the PY closure become more important, resulting in the breakdown of the HNC approximation.

B. The new closure

The new closure we propose has two ingredients. The first involves the definition of the long-range portion of the potential and the second involves estimating the contribution of the bridge function. The reader is referred to our previous work for further details.²⁵

For the new closure the long-range potential ϕ_{ab} [Eq. (2.3)] is redefined. Obviously, at large r the long-range potential should be Coulombic. Rather than defining ϕ_{ab} as a Coulomb potential for all r as is commonly done [Eq. (2.5)], we define it in a similar manner as in Andersen and Chandler,³⁵ Rogde and Hafskjold,³⁰ and Ichiye and Haymet.²⁵ In particular, ϕ_{ab} is chosen as the contribution to c due to the long-range Coulomb force in the MSA closure for charged hard spheres of radius R ,³⁶

$$\phi_{ab}(r) = \begin{cases} -\beta \frac{Z_a Z_b}{\epsilon r} \left(\frac{2Br}{R} - \frac{B^2 r^2}{R^2} \right) & r < R, \\ -\beta \frac{Z_a Z_b}{\epsilon r} & r > R, \end{cases} \quad (2.10a)$$

in which B is given by

$$B = x^{-2} [x^2 + x - x(1 + 2x)^{1/2}], \quad x^2 = \kappa^2 R^2. \quad (2.10b)$$

The renormalized function q_{ab} [Eq. (2.6)] is thus MSA chain sums rather than Debye chain sums as in Eq. (2.7) and are then given in Fourier space by

$$q_{ab}(k) = -4\pi\beta \frac{Z_a Z_b}{\epsilon [k^2 + \kappa^2 f(k)]} f(k), \quad (2.11a)$$

in which

$$\begin{aligned} f(k) = & \cos kR + \frac{2B}{kR} [\sin kR - kR \cos kR] \\ & + \left(\frac{B}{kR} \right)^2 [2(1 - \cos kR - kR \sin kR) \\ & + k^2 R^2 \cos kR]. \end{aligned} \quad (2.11b)$$

The closed-form expressions for $\phi_{ab}(r)$ and $q_{ab}(k)$ given in Eqs. (2.10) and (2.11), respectively, are a major improvement over the previous work²⁵ which involved an additional numerical step to solve them.

The second ingredient is the definition of B . The rationale for the choice of the definition is given in our previous work,²⁵ but they are slightly modified and so are defined here again. This is discussed further in Sec. V. The function B_{ab} for like charges is approximated as

$$B_{ab} = \log(1 + \tau_{ab}) - \tau_{ab}, \quad (2.12a)$$

B_{ab} for unlike charges as

$$B_{ab} = \log[2 - \exp(-\tau_{ab})(1 + \tau_{ab})]. \quad (2.12b)$$

Thus, B_{ab} for like charges is chosen such that the set of graphs which are included in the HNC expression but are ignored in the PY expression (HNC-only graphs) are also ignored, since the first bridge graph is expected to cancel the HNC-only graphs for these cases. This is because the bond connecting the black circles of the first bridge graph (see Ref. 25) is negative for repulsive forces, whether of simple van der Waals or simple hard-sphere repulsive forces, or of unlike charges as in this case. However, B_{ab} for unlike charges is chosen such that the HNC-only graphs are included twice since the first bridge graph is expected to be the same sign as the HNC-only graphs. This is because the bond connecting the black circles should be positive for unlike charges since the major contribution comes from unlike charges and is justified via comparison with numerical integrations of the first bridge graph.^{10,11} Since more than one expression with the correct first order bridge graph can be devised, other forms for the unlike charges such as

$$B_{ab} = \log(1 - \tau_{ab}) + \tau_{ab} \quad (2.13)$$

were also tried. Thus, this theory is the same as that of Rogde and Hafskjold¹² in the definition of ϕ_{ab} [Eq. (2.9)] and B_{ab}

for like charges [Eq. (2.12a)] but differs in the definition of B_{ab} for unlike charges [Eq. (2.12b)], and it is this difference which leads to the good agreement for the unlike charges.

The new integral equations thus consist of the renormalized Ornstein–Zernike equation, given by Eq. (2.6), the definition of ϕ_{ab} [Eq. (2.10)] and the new closure, given by Eq. (2.12). Since this closure consists of a PY-like equation (at least for unlike pairs) modified for ionic hard-sphere systems, we refer to it as IPY2 (to distinguish it from the earlier IPY closure²⁵).

The procedure for solving the equations is the same as given in Refs. 14 and 25, except that the new closure is used. For some ionic concentrations, simple Picard iterations seem to work better than the Newton–Raphson³⁷ scheme. The results presented below were obtained with a mesh of $N=4096$ points and $\Delta r=0.105$ Å for the electrolytes and $N=2048$ points and $\Delta r=0.0125$ Å for the molten salt. All results were converged sufficiently so that the zeroth moment condition was satisfied to within $1\times 10^{-4}\%$ or better and the second moment condition was satisfied to within $5\times 10^{-3}\%$ or better.

III. SIMULATIONS

MC simulations of dilute primitive 2:2 electrolytes have been performed to compare with the integral equation theory predictions. In each case, the systems consist of $N=108$ particles, with $N/2$ positive ions and $N/2$ negative ions of absolute charge $2e$, enclosed in a cubical box whose size is adjusted to obtain the proper electrolyte concentration. The interparticle potential function is given in Eq. (2.4). The positive and negative ions are chosen to be of the same size, as in the integral equation calculations, with $R=4.2$ Å. The usual Metropolis algorithm³³ is used to sample the configurations in canonical ensemble (NVT) at a temperature $T=298.16$ K, unless otherwise specified. Periodic boundary conditions are used to minimize the surface effects and the electrostatic interactions are truncated using the minimum image convention. The use of Ewald sums to treat the Coulomb interactions accurately is not required in the case of dilute electrolyte solutions since $\kappa L \gg 1$ (with L being the side length of the cubic simulation box) and the packing fraction is too low for the systems studied, thus resulting in negligible boundary condition effects. For the molten salt case, the MC data of Larsen¹³ were used and so no simulations were performed here at those concentrations. The maximum displacement for a particle is adjusted in such a way that the acceptance ratio for a trial move is 0.5.³⁴ In all the electrolyte concentrations studied, it is observed that a trial move of roughly $0.08 L$ gave this ratio (Table I).

There was some difficulty in obtaining good statistics for the like charge pair distribution functions between R and $3R$ at 0.005 M because the like ion population at these separations is negligible. While biasing such as umbrella sampling^{38,39} is often used, the evaluation of the proportionality constant needed to get the true $g(r)$ from the biased one was found to be difficult in earlier simulations of the same systems^{10,11} using umbrella sampling. Also, MD simulations for the same model at 0.005 M⁴⁰ showed marked deviations from the biased MC data of Rossky and co-workers.^{10,11}

TABLE I. Details of the MC simulations for the dilute electrolyte solution regime. $N=108$ with $N/2$ positive and $N/2$ negative ions of absolute charge $2.0e$.

C_{ST} (M)	Box length	
	L (Å)	Displacement for acceptance ratio of 0.5 (Å)
0.005	261.74	20.00
0.0625	112.78	9.59
0.20	76.53	5.66
0.50	56.39	4.63
1.50	39.10	3.33

When similar biasing for a 0.005 M simulation was used here, the accuracy of the results was found to be dependent on the distance range of the bias. Thus, the 0.005 M simulation reported here used no bias but instead employed 2×10^6 trial moves per particle after equilibration. For the rest of the simulations, 10^5 trial moves per particle were employed after equilibration. The $g(r)$ data was collected on a fine grid of 0.025 Å and the data for like charges was further smoothed by taking averages of points within 0.1 Å grid in a way similar to spectral analysis. The $g(r)$ data at the important region between R and $3R$ was thus obtained with reasonable statistics.

IV. RESULTS

A. Structure of 2:2 aqueous electrolytes in the primitive model

In this section, our IPY2 and MC results are compared for the same model systems, namely, the primitive model with $R=4.2$ Å, charge of $\pm 2e$, and solvent dielectric constant $\epsilon=78.358$. The corresponding HNC results are also shown. The temperature T is kept at 298.16 K unless otherwise specified.

At a concentration of 0.005 M ($\kappa R=0.20$), the IPY2 results for g_{++} are much closer to the Monte Carlo data than the simple HNC (Fig. 1). The most important feature is that

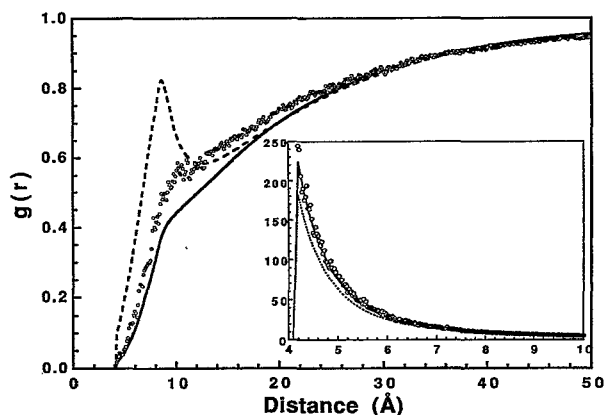


FIG. 1. Like charge pair correlation functions for 0.005 M aqueous 2–2 electrolyte solution. Inset shows the corresponding unlike charge distribution functions. Solid line is for IPY2, dashed line is for HNC, and circles are for MC.

TABLE II. The heights of first peaks in the unlike charge distribution functions for various electrolyte concentrations and a molten salt.

Concentration (M)	κR	IPY2	HNC	MC
0.005	0.20	224.21	181.76	244.80
0.0625 ^a	0.69	47.31	37.94	45.48
0.20	1.24	19.69	18.70	17.93
0.50	1.95	10.83	10.64	9.01
1.50	3.39	5.95	5.95	4.57
Molten salt	17.27	13.05	14.22	13.25 \pm 0.50 ^b

^aData at 303 K.^bData from Ref. 13.

the IPY2 results are a monotonically increasing function of r so that the unusual peak at $r=2R$ in HNC is absent in the IPY2 data, in agreement with the MC data. Besides this peak, for $r < 2R$, the MC curve lies between the HNC and IPY2 but is closer to the IPY2, especially at contact. For larger r , the two integral equations are slightly below the MC data, merging with the MC data after 25 Å. Close examination of the MC results reveals a small bump at $r=2R$, which is also apparent in IPY2 results. However, the HNC approximation highly overestimates the peak resulting in the non-monotonic behavior, an artifact of the theory which is corrected in the new closure. Both integral equations (IPY2 and HNC) and MC results for g_{+-} of the hard spheres are very similar, and vary mainly in the height of the peak at $r=R$ (Fig. 1, inset). The MC shows a peak height of 245 (Table II). Both the integral equations underestimate the peak height but the IPY2 peak height is significantly higher than the HNC peak height and is very close to the MC data (Table II). In comparison to the soft-sphere IPY theory²⁵ at 0.005 M, both IPY and IPY2 showed similar improvement over HNC for the like charge distribution function. However, IPY significantly overpredicted the MC for unlike distribution function, so that IPY2 theory exhibits a marked improvement over IPY.

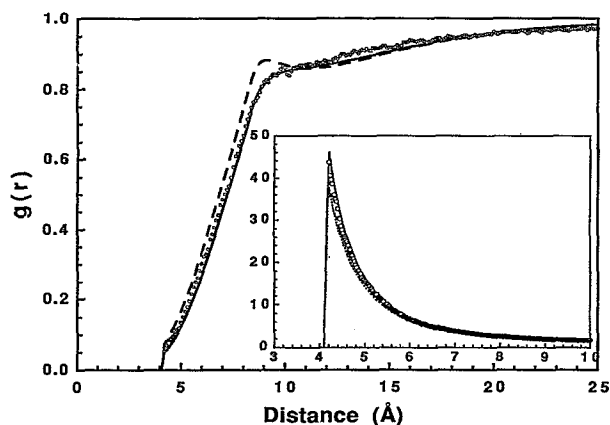


FIG. 2. Like charge pair correlation functions for 0.0625 M aqueous 2-2 electrolyte solution at 303 K. Inset shows the corresponding unlike charge distribution functions. Symbols as in Fig. 1.

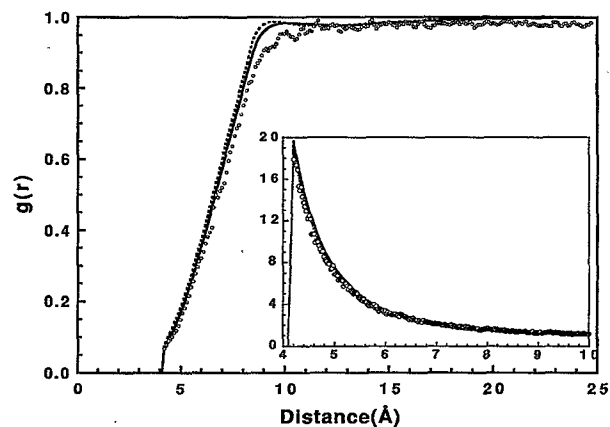


FIG. 3. Like charge pair correlation functions for 0.2 M aqueous 2:2 electrolyte solution. Inset shows the corresponding unlike charge distribution functions. Symbols as in Fig. 1.

The results for 0.0625 M ($\kappa R=0.69$) solution are shown in Fig. 2. At this concentration, we were unable to obtain convergence for the IPY2 at 298 K and thus the results are shown at 303 K. For the like charge distribution functions, the IPY2 and MC results are very close (Fig. 2). Once again, the HNC closure shows clear nonmonotonic behavior which is absent in MC and IPY2 data. Even though the IPY2 results are closer to the MC data near contact and at larger distances (Fig. 2), IPY2 data do show a slight deviation from the monotonic behavior at $r > 2R$, a feature absent in the MC data. It appears that the integral equations predict too early the features of distribution functions at higher electrolyte concentrations where the like charge correlation functions are nonmonotonic, which is discussed further below. The unlike charge correlation functions predicted by IPY2 is very close to the MC data (Fig. 2, inset) as in the case of 0.005 M. The IPY2 peak height is higher than the MC peak by two units and the HNC peak was lower than the MC peak by six units (Table II, Fig. 2, inset). In comparison to the soft-sphere IPY theory,²⁵ IPY2 theory exhibits a marked improvement in the like charge distribution functions in that both HNC and IPY results were far below the MC data with the IPY results lying below the HNC data. The soft-sphere IPY results for the unlike charges showed identical trends with the present hard-sphere IPY2 theory.

The integral equation results for g_{++} at a concentration of 0.2 M ($\kappa R=1.24$) are all quite similar to each other and to the MC results except for a small region near $2R$ where the MC data is slightly below the theory results (Fig. 3). Again, the IPY2 result is closer to the MC data. At this concentration, the nonmonotonicity, which is a feature of like charge distribution functions in higher electrolyte concentrations, is clearly identifiable for the integral equation results. However, the MC data show no such behavior at this concentration. The heights of the g_{+-} correlation functions at 0.2 M are almost identical with MC, IPY2, and HNC giving 17.93, 19.69, and 18.70, respectively (Fig. 3, inset, Table II). For the soft-sphere case studied in Ref. 25, the IPY integral equation results showed identical trends as the hard-sphere IPY2

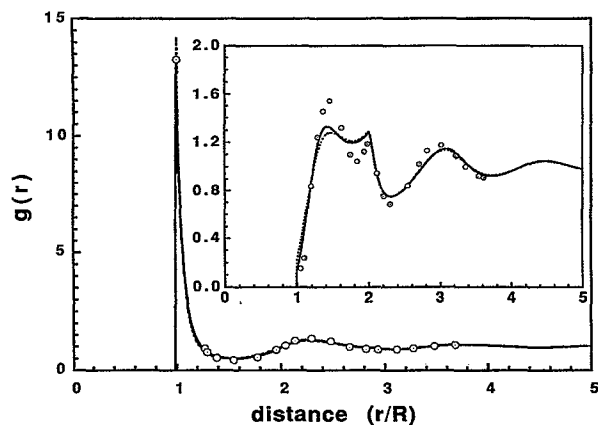


FIG. 4. Unlike charge pair correlation functions for a molten salt. Inset shows the corresponding like charge distribution functions. Symbols as in Fig. 1. The MC data is taken from Ref. 13.

results. However, the MC results for the like charge functions were above the theory results in the distance range from R to $3R$.

Very high concentrations of salts were also studied. At 0.50 and 1.50 M, both like and unlike distributions from IPY2, HNC, and MC are very similar and so are not shown. The peak heights for the unlike distributions are given in Table II, which shows that IPY2 approaches HNC in this limit, and both integral equation theories give slightly higher results than MC.

B. Ionic distributions in molten salts

The IPY2 closure for a hard-sphere model in the molten salt regime was solved for the same thermodynamic state conditions as in Ref. 24 for which MC data is available for comparison.¹³ The state parameters are $\rho^* = \rho R^3 = 0.669$ and $\beta^* = (Ze)^2 / \epsilon k_B T R = 35.476$. For $\epsilon = 1$, $R = 1$, and $Z = \pm 1$, this corresponds to a hard-sphere molten salt at $T = 4710.85$ K with $\kappa R = 17.27$. The converged solutions using the IPY2 closure relation in this model indicate that the like charge distribution functions are close to the HNC data but with again a slight improvement for the first peak height as compared to the MC data (Fig. 4, inset). For the unlike charges, the IPY2 peak height is almost identical with the corresponding MC data of Larsen¹³ (Fig. 4, Table II) whereas HNC predicts a somewhat higher peak. The MHNC calculations,²⁴ in which hard-sphere bridge functions with varying hard-sphere diameters are used, showed marked improvement for the first peak of the like distribution function and showed unlike charge peak height in agreement with MC data. However, the prediction for the second peak showed no improvements and is virtually identical with the HNC and IPY2 data. Moreover, the MHNC involves varying the hard-sphere reference diameters to get a good fit and thus has no predictive value. The RHNC calculations²⁴ in which hard-sphere bridge functions are used, gave results similar to HNC. In addition, IPY2 results for the molten salts showed a greater improvement over HNC than the soft-sphere IPY results.⁴¹

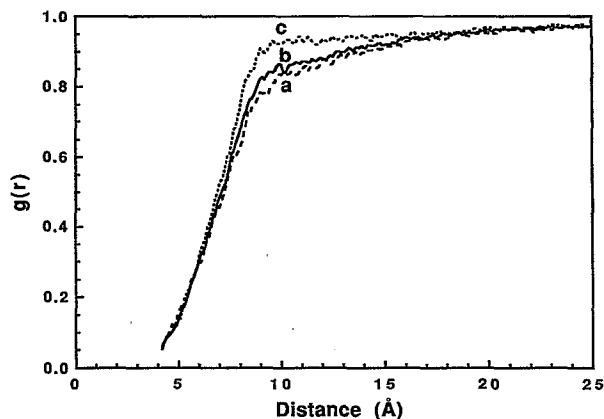


FIG. 5. The MC results for like charge distribution functions at 0.0625 M solution at three different temperatures. Curve "a" is the data at 315 K, curve "b" is the data at 303 K, and curve "c" is the data at 275 K.

C. Transition from monotonic to nonmonotonic behavior in the like distribution functions

The transition from monotonic to nonmonotonic behavior in the like charge distribution functions with increasing concentrations is of interest as it indicates the onset of formation of ion clusters with more than two ions. As the concentration increases to the molten salt regime, the like distribution functions become oscillatory. In this section, this transition is investigated, along with the problems in convergence for the IPY2 closure which appears to be associated with the onset of nonmonotonic behavior.

The problems in convergence for the IPY2 closure as temperature was decreased below 303 K at 0.0625 M appear to be related to the behavior at $r = 2R$. To investigate this further, MC simulations at three different temperatures at this concentration have also been performed. In Fig. 5, the like charge ion distribution functions obtained from MC simulations at temperatures 275 ($\kappa R = 0.72$), 303 ($\kappa R = 0.69$), and 315 K ($\kappa R = 0.67$) are shown. The distribution functions are smooth and monotonic although at $T = 275$ K there seems to be slight tendency for nonmonotonic behavior at $r < 2R$.⁴² However, the IPY2 results at 315 ($\kappa R = 0.67$) and 303 K ($\kappa R = 0.69$) show a different behavior near $r = 2R$ (Fig. 6) in that the results at 315 K are purely monotonic and the results at 303 K are nonmonotonic as discussed previously. Below 303 K, the IPY2 equations failed to converge. The corresponding HNC results (Fig. 6) show nonmonotonic behavior even at 315 K, and although HNC converges at 298 K, there is a very obvious peak at $r = 2R$ which is not evident in the MC as discussed above. We believe that the problems in convergence for the IPY2 closure at temperatures below 303 K are related to the onset of the peak at $r = 2R$, i.e., the region where a transition occurs from monotonic behavior at a higher temperature to a nonmonotonic behavior at lower temperatures. It appears that this transition occurs below 275 K in the MC (Fig. 5), around 303 K in the IPY2 (Fig. 6), and above 315 K in the HNC (Fig. 6).

The nonmonotonic behavior in the like distributions at 0.2 M (Fig. 3) seen in the IPY2 but not in the MC was also

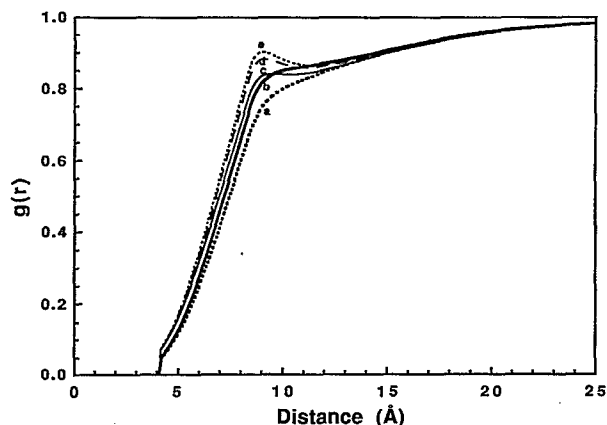


FIG. 6. The IPY2 and HNC results for the like charge distribution functions at 0.0625 M solution at different temperatures. Thick dots (curve a) are the IPY2 data at 315 K, thick line (curve b) is the data at 303 K. Thin line (curve c) is for HNC data at 315 K, thin dashed line (curve d) is for HNC data at 303 K, and thin dotted line (curve e) is for HNC data at 298 K.

investigated. Although the MC shows monotonic behavior at 0.2 M, at higher concentrations of 0.5 and 1.5 M (Fig. 7), the MC data do show nonmonotonic behavior. The corresponding IPY2 data is also shown in Fig. 7 for comparison. The IPY2 peak heights are higher than the MC results. The HNC results are almost identical with the IPY2 results and thus are not shown in Fig. 7. Evidently, the integral equations predict too early the features of distribution functions in strong electrolytes at intermediate concentrations.

The failure of IPY2 to converge was further studied by solving the IPY2 closure for a range of concentrations from 0.001 to 1.5 M at 298 K ($\kappa R = 0.09$ to $\kappa R = 3.39$). The results for the like charge correlation functions are shown in Fig. 8. The nonmonotonic behavior is clearly visible at 0.08 M ($\kappa R = 0.78$) and above and is clearly monotonic at 0.005 M ($\kappa R = 0.20$) and below. In between 0.08 and 0.005 M, the range for the transition between these two kinds of behaviors, the IPY2 closure failed to converge. At higher temperatures, this

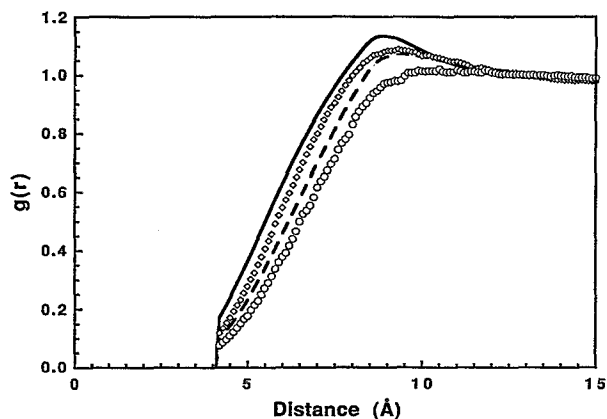


FIG. 7. The IPY2 and MC results for the like charge distribution functions for the 2:2 aqueous electrolyte at 1.5 and 0.5 M at 298 K. The dashed and thick lines represent the IPY2 data at 0.5 and 1.5 M, respectively. The circles and squares are the corresponding MC data.

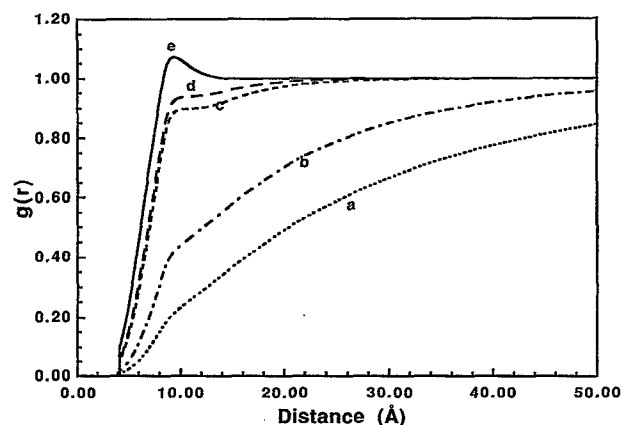


FIG. 8. The IPY2 closure results for the like charge distribution functions for the 2:2 aqueous electrolyte solution at various concentrations starting from 0.001 to 0.5 M at 298 K. Dotted line (curve a) is at 0.001 M and $\kappa R = 0.09$, dot-dashed line (curve b) is for 0.005 M and $\kappa R = 0.20$, short dashed line (curve c) is for 0.08 M and $\kappa R = 0.78$, long dashed line (curve d) is for 0.128 M and $\kappa R = 0.99$, and thick line (curve e) is for 0.5 M and $\kappa R = 1.95$.

range is expected to become narrower from the discussions presented above. Thus at 303 K, the transition region for the IPY2 closure is between 0.0625 ($\kappa R = 0.69$) and 0.007 M ($\kappa R = 0.23$) and at 308 K, the region is even smaller and it occurs between 0.01 and 0.05 M.

The temperature and concentration (via κR) dependence of the transition from monotonic to nonmonotonic behavior in the like distributions and the failure to converge were investigated for the IPY2 closure (Fig. 9). Figure 9 may be viewed as a phase diagram where the temperature vs κR below which the IPY2 equations failed to converge is plotted. There are three different types of behavior seen. In region a, i.e., at low densities or κR , the like charge functions are purely monotonic. In region b, i.e., at higher densities or

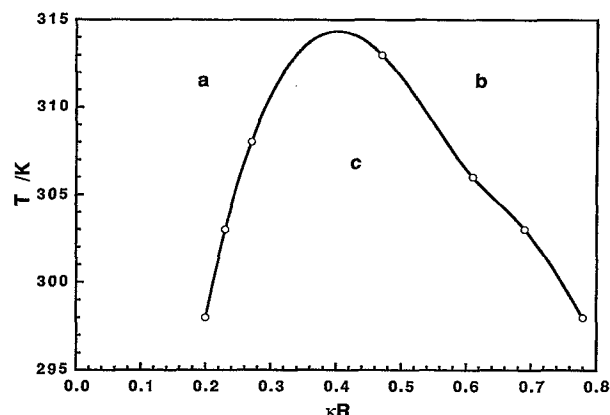


FIG. 9. Temperature vs κR plot for 2:2 aqueous electrolytes showing the region where the IPY2 equations failed to converge. Circles represent the lowest temperature at which the solution can be found for a given value of κR and the solid line is a cubic spline fit to those points. Region a outside the curve is the region where monotonic behavior for the like charge correlation function dominates. Region b is the region where nonmonotonicity dominates. Below the curve (region c) the IPY2 equations failed to converge.

κR , the functions are purely nonmonotonic. Below this curve in region c, the IPY2 equations are not convergent. This is the region where a transition occurs between monotonic behavior in which ion pairing is important to a nonmonotonic behavior in which there is a tendency for ionic clustering. At still higher concentrations or κR , one would expect another region where the distribution functions become oscillatory,⁴³ because the ions form clear coordination shells. From Fig. 9, it is clear that κR around 0.4 (which corresponds to concentrations around 0.02 M for aqueous 2:2 electrolytes) is critical for the IPY2 closure so that IPY2 solutions exist only at higher temperatures (above 314 K). The curve resembles a spinodal under which the IPY2 closure has no solution. For the HNC closure, one cannot anticipate such a transition region because the observed distribution functions are nonmonotonic at even extremely low concentrations as in the case of 0.005, which corresponds to $\kappa R=0.20$ (Fig. 1). However, we expect that one can observe such a transition region in a simulation even though the critical concentration predicted by the simulation will be higher than that predicted by the IPY2 theory (as evident from Figs. 5 and 7).

V. DISCUSSION AND CONCLUSIONS

The new closure presented here has two main ingredients. The first is the definition of the long-range potential $\phi_{ab}(r)$ which is defined as in the works of Andersen and Chandler³⁶ and Rogde and Hafskjold¹² for hard-sphere repulsive forces. The second ingredient in the closure is the form of the closure itself. For the like charges, the closure is identical to that of Rogde and Hafskjold.¹² However, the closure for unlike charges has a very different form and is similar to that of Ichiye and Haymet.²⁵ This essential difference results in bridge functions which are in agreement with the numerically evaluated first bridge graph.¹¹

There is one change in the form of the closure for unlike charges from the previous work.²⁵ In that work, B_{ab} for unlike charges was approximated as Eq. (12b) for $\tau_{ab}<0$ but as Eq. (2.12a) for $\tau_{ab}>0$. This choice was motivated by examining the form of B_{ab} for molten salts. In addition, Duh and Haymet³² have made a choice of the form for B_{ab} based solely on the sign of τ_{ab} and not on whether a and b are like or unlike. Although this choice was based on evaluation of B_{ab} and τ_{ab} from simulations, we feel this is not particularly meaningful since for the concentration ranges chosen (i.e., electrolytes), $\tau_{ab}<0$ for unlike charges and $\tau_{ab}>0$ for like charges for all values of τ_a which are significantly nonzero. Thus, whether the definition of B_{ab} based on the Duh and Haymet conditions³² or whether $a=b$ or $a\neq b$, the resulting bridge functions are essentially same for the electrolyte regime. We have also tried the conditions given by Duh and Haymet³² and in the previous work²⁵ for the hard-sphere cases given here. For the electrolytes, these results are identical to those with the conditions given in Eq. (2.12) as to be expected. For molten salts, the results using the Ichiye and Haymet conditions²⁵ are essentially identical to those with Eq. (2.12), while the results for the Duh and Haymet conditions are worse.³² Thus, the separation based on the sign of τ_{ab} for unlike charges which we originally proposed in the previous work²⁵ in hopes of improving the molten salts

makes no difference for unlike charges and is thus an unnecessary complication and makes the like charge results worse for molten salts. For this reason, and because we can graphically rationalize our choice to define B_{ab} based whether $a=b$ or $a\neq b$, we prefer the conditions as given in Eq. (2.12).

Overall, the results presented here for the IPY2 closure represent a considerable improvement over the HNC closure for dilute strong electrolytes. The most characteristic feature of the unlike charge distributions is the peak height. At electrolyte concentrations of 0.005 and 0.0625 M, IPY2 is significantly better than HNC at predicting the peak height for the unlike charges. At higher concentrations of 0.2 and 0.5 M, IPY2 is slightly worse than HNC at predicting the peak height for the unlike charges, but IPY2 approaches HNC at 1.5 M. For molten salts, both IPY2 and HNC are within one unit of the MC peak height but in this case the IPY2 is closer. These results indicate that the choice of adding the canceling PY-like bridge graphs twice for unlike charges is important. There are two characteristic regions of the like charge distribution: near contact and near $r=2R$. For all cases of the electrolytes and the molten salt, IPY2 predicted the contact region better than HNC. The results for IPY2 near $r=2R$ were better than HNC for the electrolytes at 0.005, 0.0625, and 0.2 M and for molten salts. The most significant improvement of IPY2 was correctly predicting a monotonic increase with r at 0.005 M, whereas HNC incorrectly predicts a peak at $r=2R$. These results indicate that the choice of a PY-like approximation for like charges is reasonable. Thus, over a wide range of concentrations of strong electrolytes and for the molten salt regime, IPY2 appears to generally improve over the HNC theory for ionic liquids.

The hard-sphere IPY2 closure also represents an improvement over the original soft-sphere IPY closure. Because there are closed-form expressions for ϕ and q , the IPY2 closure for hard spheres is much simpler than that for soft spheres, which required an additional step of solving the soft-sphere MSA closure. Thus, it requires essentially no more computation time than solving the renormalized HNC closure. Moreover, the hard-sphere IPY2 closure generally gave improvement over HNC greater than or equal to the corresponding IPY closure results for soft spheres. A significant improvement found in the hard-sphere IPY2 closure is that it gives better results than HNC both in the molten salt as well as in the dilute solution regimes, whereas the soft-sphere IPY closure gave the same results as HNC in the molten salt regime.⁴¹

Finally, using the IPY2 closure, we have identified a clear cut region of temperatures and κR in the dilute electrolyte solution regime where a transition occurs between monotonic and nonmonotonic behaviors in the like pair distribution functions. In this critical region, the IPY2 equations failed to converge at lower temperatures. The transition must occur in a somewhat different region in the MC simulation, apparently below 275 K at 0.0625 M ($\kappa R=0.72$) and about at 298 K at 0.5 M ($\kappa R=1.95$). The location of such a transition region for HNC is unclear as nonmonotonic behavior is observed at all concentrations and temperatures studied,

although a comprehensive search was not made. In particular, the HNC like pair correlation functions show a pronounced peak at low concentrations at 298 K which is corrected in the new IPY2 closure. Thus it appears that the transition region predicted by IPY2 occurs in the MC, but in a slightly different region, and must be in a very different region if at all in HNC. The nature of this transition is being investigated further in MC simulations.

ACKNOWLEDGMENTS

This research was supported in part by grants from the (U.S.) National Science Foundation (MCB-9118085), the American Chemical Society–Petroleum Research Foundation (23983-G6), and in part by funds provided by Washington State University. We also thank the VADMS Laboratory at WSU for computational resources.

- ¹R. D. Cannon, *Electron Transfer Reactions* (Butterworths, London, 1980).
- ²H. L. Friedman, *Faraday Discuss. Chem. Soc.* **85**, 1 (1988).
- ³C. Ghelis and J. Yon, *Protein Folding* (Academic, New York, 1982).
- ⁴L. S. Ornstein and F. Zernike, *Proc. Akad. Sci. (Amsterdam)* **17**, 793 (1914).
- ⁵H. L. Friedman and B. Larsen, *Pure Appl. Chem.* **51**, 2147 (1979), and references therein.
- ⁶H. L. Friedman, *Annu. Rev. Phys. Chem.* **32**, 179 (1981).
- ⁷J. P. Hansen and I. R. McDonald, *Theory of Simple Liquids*, 2nd ed. (Academic, New York, 1986).
- ⁸J. S. Høye, E. Lomba, and G. Stell, *Mol. Phys.* **79**, 523 (1993), and references therein.
- ⁹J. P. Hansen and I. R. McDonald, *Phys. Rev. A* **11**, 2111 (1975).
- ¹⁰P. J. Rossky, J. B. Dudowicz, B. L. Tembe, and H. L. Friedman, *J. Chem. Phys.* **73**, 3372 (1980).
- ¹¹R. Bacquet and P. J. Rossky, *J. Chem. Phys.* **79**, 1419 (1983).
- ¹²S. A. Rogde and B. Hafskjold, *Mol. Phys.* **48**, 1241 (1983).
- ¹³B. Larsen, *J. Chem. Phys.* **68**, 4511 (1978).
- ¹⁴T. Ichiye and A. D. J. Haymet, *J. Chem. Phys.* **89**, 4315 (1988).
- ¹⁵R. A. Thuraisingham and H. L. Friedman, *J. Chem. Phys.* **78**, 5772 (1983).
- ¹⁶H. L. Lemberg and F. H. Stillinger, *J. Chem. Phys.* **62**, 1677 (1975).
- ¹⁷F. H. Stillinger, *Israel J. Chem.* **14**, 130 (1975).
- ¹⁸H. L. Lemberg and F. H. Stillinger, *Mol. Phys.* **32**, 353 (1976).
- ¹⁹F. H. Stillinger and A. Rahman, *J. Chem. Phys.* **68**, 666 (1978).
- ²⁰J. M. J. van Leeuwen, J. Groeneveld, and J. deBoer, *Physica* **25**, 792 (1959).
- ²¹Y. Rosenfeld and N. W. Ashcroft, *Phys. Rev. A* **20**, 1208 (1979).
- ²²F. Lado, *Phys. Rev. A* **8**, 2548 (1973).
- ²³F. Lado, S. M. Foiles, and N. W. Ashcroft, *Phys. Rev. A* **28**, 2374 (1983).
- ²⁴C. Caccamo, G. Malescio, and L. Reatto, *J. Chem. Phys.* **81**, 4093 (1984).
- ²⁵T. Ichiye and A. D. J. Haymet, *J. Chem. Phys.* **93**, 8954 (1990).
- ²⁶H. Iyetomi and S. Ichimaru, *Phys. Rev. A* **27**, 33,241 (1983).
- ²⁷J. Rescic, V. Vlachy, and A. D. J. Haymet, *J. Am. Chem. Soc.* **112**, 3398 (1990).
- ²⁸W. G. Madden, *J. Chem. Phys.* **75**, 1984 (1981).
- ²⁹A. R. Allnatt, *Mol. Phys.* **8**, 533 (1964).
- ³⁰S. A. Rogde and B. Hafskjold, *Acta Chem. Scand. Ser. A* **35**, 263 (1981).
- ³¹V. Vlachy, T. Ichiye, and A. D. J. Haymet, *J. Am. Chem. Soc.* **113**, 1077 (1991).
- ³²D.-M. Duh and A. D. J. Haymet, *J. Chem. Phys.* **97**, 7716 (1992).
- ³³M. Metropolis, A. W. Rosenbluth, M. N. Rosenbluth, A. N. Teller, and E. Teller, *J. Chem. Phys.* **21**, 1087 (1953).
- ³⁴M. P. Allen and D. J. Tildesley, *Computer Simulation of Liquids* (Oxford University, Oxford, 1992).
- ³⁵H. C. Andersen and D. Chandler, *J. Chem. Phys.* **57**, 1918 (1972).
- ³⁶E. Waisman and J. L. Lebowitz, *J. Chem. Phys.* **56**, 3093 (1972).
- ³⁷S. Labik, A. Malijevsky, and P. Vonka, *Mol. Phys.* **56**, 709 (1985).
- ³⁸G. N. Patey and J. P. Valleau, *J. Chem. Phys.* **63**, 2334 (1975).
- ³⁹C. Pangali, M. Rao, and B. J. Berne, *J. Chem. Phys.* **71**, 2975 (1979).
- ⁴⁰D. Smith, Yu. V. Kalyuzhnyi, and A. D. J. Haymet, *J. Chem. Phys.* **95**, 9165 (1991).
- ⁴¹T. Ichiye (unpublished results).
- ⁴²V. Vlachy (personal communication).
- ⁴³P. Attard, *Phys. Rev. E* **48**, 3604 (1993).